

RESEARCH ARTICLE OPEN ACCESS

Green Electrochromic Film Formation via Phenylcarbazole Polymerization in Ionic Liquids

 Carolina Gascó¹ | Sara Santiago² | Rosa Maria Sebastián¹ | Gonzalo Guirado¹
¹Departament de Química, Universitat Autònoma de Barcelona, Barcelona, Spain | ²Department of Materials and Environmental Chemistry, Stockholm University, Stockholm, Sweden

Correspondence: Rosa Maria Sebastián (rosamaria.sebastian@uab.cat) | Gonzalo Guirado (gonzalo.guirado@uab.cat)

Received: 3 February 2026 | **Revised:** 4 April 2026 | **Accepted:** 9 April 2026

Keywords: electrochromic polymer | flexible electrochromic displays | green electrosynthesis | ionic liquid | polycarbazole derivatives

ABSTRACT

The scale-up of electrochromic devices (ECD) from laboratory research to mass production is still challenging due to the use of toxic organic solvents and electrolytes, as well as performance losses when transferred to solid substrates specially flexible ones. Here, we present a green approach for the electropolymerization of polycarbazoles on flexible substrates, using two distinct monomers: 4-(9*H*-carbazol-9-yl)phenol and 4-(3-methoxy-9*H*-carbazol-9-yl)phenol. 1-Butyl-3-methylimidazolium bis(trifluoromethylsulfonyl)imide (BMIM-TFSI) ionic liquid (IL) is used as a reusable electrolyte medium, which not only minimizes environmental impact but also enables efficient modulation of the electrochromic performance. The resulting electroactive films showed promising coverage ($2.24 \cdot 10^{-9}$ and $2.5 \cdot 10^{-8}$ mol cm⁻², respectively), and efficient electrochromic features (31 and 17 cm² C⁻¹, respectively), demonstrating their potential for improving sustainable fabrication protocols and paving the way toward practical, environmentally friendly ECD applications.

1 | Introduction

The dynamic modulation of optical properties of functional materials, especially the colour, through external stimuli has become a promising strategy for the design of smart devices. Among different stimuli, current or electric voltage has demonstrated notable advantages due to its precise control, low power requirements, and feasible integration into electronic systems.

The reversible change in the absorbance or transmittance in the visible or near-IR wavelength range when an electric stimulus is applied is known as electrochromism and is the result of electronic transitions between oxidized and reduced states of electroactive species [1–6]. The fundamental mechanisms of electrochromism and the implementation of organic materials have been widely reported, highlighting their reversible modulation of optical properties as a key feature for smart optical applications

[5]. Recent advances in electrochromic materials have been boosted by the growing demand for sustainable, portable, and flexible systems, especially in emerging applications such as wearable sensors, smart textiles, and highly efficient displays. However, closing the gap between high-performance materials developed at the laboratory scale and their application in practical devices remains a central challenge.

Conjugated conducting polymers are considered one of the most relevant families of electrochromic materials because of their exceptional electronic conductivity with structural and chemical tunability. These materials present a conjugated bond system that allows charge delocalization and improves redox efficiency, thereby strengthening their electrochemical and optical responses. Some benchmark conducting polymers examples are poly(3,4-ethylenedioxythiophene) (PEDOT) and polyaniline (PANI) which demonstrate high conductivity

This is an open access article under the terms of the [Creative Commons Attribution-NonCommercial](https://creativecommons.org/licenses/by-nc/4.0/) License, which permits use, distribution and reproduction in any medium, provided the original work is properly cited and is not used for commercial purposes.

© 2026 The Author(s). *Chemistry – A European Journal* published by Wiley-VCH GmbH

and electrochemical stability and are considered as reference systems for electrochromic applications devices [7]. Moreover, electroactive polymers have expanded toward multifunctional and more complex architectures that integrate optical transparency, mechanical flexibility, and environmental stability, enabling their use in flexible electronics and smart systems [8]. Because of this, research in electrochromic conducting polymers continues to expand with the aim of improving the performance of current ECDs and smart systems.

The molecular tunability, the efficient charge transport, and enhanced electrochromic performance have positioned *N*-phenylcarbazole (NPC) polymers as one of the most promising families of electrochromic materials. NPC units are known to form stable radical cations upon anodic oxidation, enabling fast switching between oxidized and nonoxidized states and high coloration efficiency. Additionally, NPC-based polymers show strong absorption in the near-infrared (NIR) range when oxidized at low potentials, which is attributed to intervalence charge-transfer (IV-CT) bands [9–11]. This characteristic is particularly advantageous for applications that require NIR shielding, such as thermal regulation in medical devices, aerospace coatings, and military camouflage [12–14]. These properties position NPC-based polymers as potential materials that fill the gap between fundamental materials science and application developments [15].

In particular, the tunability of NPC-based polymers enables the achievement of superior features such as high solubility optical transparency and multi-colored material and improved electrochemical reversibility and stability as a thin solid film for its implementation in feasible applications [16, 17]. In this sense, NPCs have been incorporated as pendant electroactive moieties in various polymer architectures, including polyphenylene ether [18] and polyacetylene [19].

Several methodologies to obtain NPC-based polymers have been exhaustively explored. However, from a sustainability perspective, electrochemical techniques are considered environmentally cleaner as they allow for the electropolymerization of NPC monomers in a one-step process thereby reducing hazardous reagents and energy consumption. Besides, electrochemical polymerization has been traditionally carried out using organic solvents such as acetonitrile, dichloromethane or propylene carbonate, although these solvents show several drawbacks (e.g. volatility, flammability, high toxicity and recyclability). In this sense, ionic liquids (ILs) have demonstrated to be an efficient alternative due to their unique physicochemical and environmental benefits. ILs are composed entirely of ions that allow them to function simultaneously as both, solvent and supporting electrolyte reducing the use of chemicals. In addition, due to their wide electrochemical window and high ionic conductivity in mild conditions, they have emerged as an ideal media for uniform electrochromic polymer film growth on conductive substrates [20]. Apart from improving the sustainability of the process by offering a recyclable medium, ILs enable precise control over polymer film growth and properties, improving electrochemical stability, faster switching times, and improved coloration efficiency compared with those synthesized in conventional molecular solvents [21, 22]. Furthermore, this approach allows the formation of thin, flexible solid films on conductive substrates such as ITO-PET

showing excellent mechanical properties including flexibility without compromising its electrochromic performance [2, 23–27].

These approaches support the fabrication of thin, flexible electrochromic films with enhanced mechanical properties and device compatibility [28–30]. Furthermore, advances in electropolymerization of stable electrochromic polymers, electrodeposition, and device integration continue to expand their potential for practical applications in smart and sustainable technologies [30].

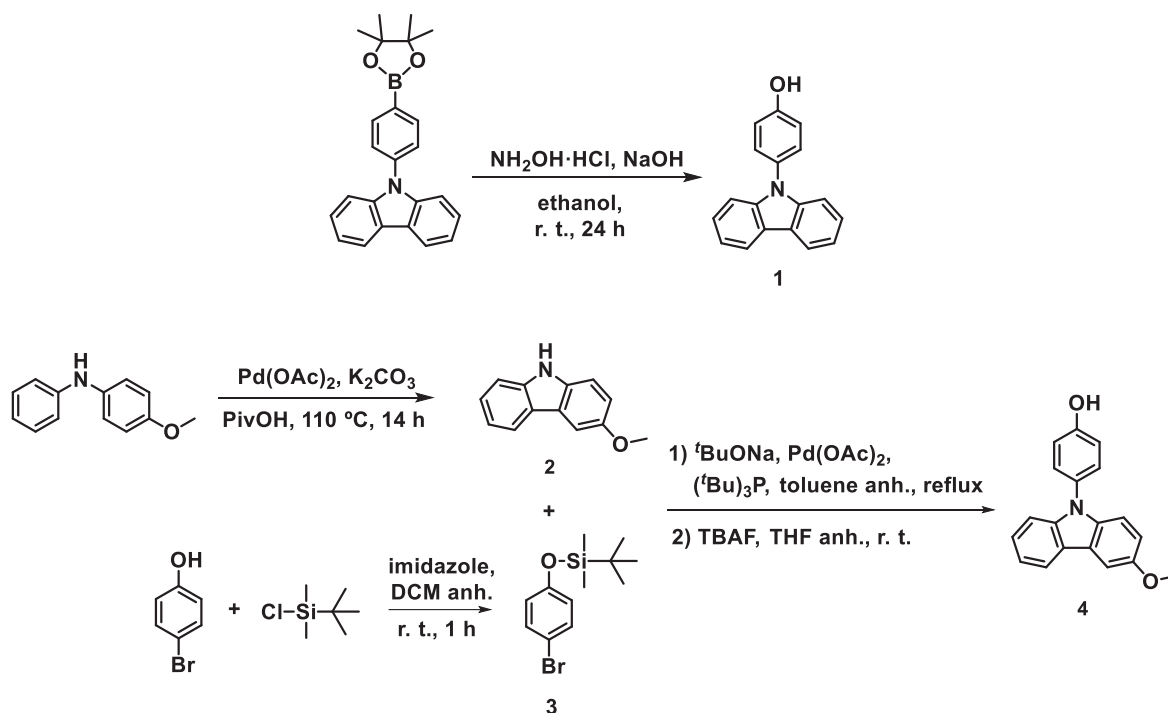
This study focused on the assisted electropolymerization of *para*-substituted NPC-based polymers on flexible ITO-PET substrates using 1-butyl-3-methylimidazolium bis(trifluoromethylsulfonyl)imide (BMIM-TFSI) electrolyte. The influence of electron-donating substituents on redox behaviour, electrochemical stability, and electrochromic performance was systematically investigated through electrochemical and spectroelectrochemical characterization of the resulting polymers. This one-step and greener electropolymerization method allowed direct synthesis on electrodes and produces polymers with excellent mechanical properties, offering a versatile approach for fabricating high-performance electrochromic materials. Finally, we demonstrated a flexible electrochromic prototype using a BMIM-TFSI gel electrolyte, highlighting the potential for integration into flexible, sustainable and portable smart systems.

2 | Experimental

2.1 | Materials and Measurements

Reagents used for the synthesis of *N*-phenylcarbazoles were of high purity and used as received from Merck. High-purity grade (< 99%) organic solvents were used for synthesis and were obtained from Across. BMIM TFSI (pur. 99.9%) from Solvionic. Prior to use, all solvents were dried using molecular sieves (3–4 Å) following standard protocols [31]. Electrochemical characterization in a solution system, was carried out using a conical cell at 22 °C for a three-electrode setup consisting of an ITO-PET working electrode (WE) (1.2 cm² electroactive area), an external platinum bar counter electrode (CE), and a saturated calomel reference electrode (SCE) isolated from the WE by a salt bridge filled with the electrolyte solution. Electrodeposition, cyclic voltammetry (CV), and chronoamperometry (CA) measurements were performed using the same set-up in BMIM-TFSI supporting electrolyte using a CHI Instrument Electrochemical (potentiostat model CHI600E) and controlled by CHI for data acquisition and treatment.

The spectroelectrochemical measurements of the modified ITO-PET were first carried out employing a 0.1 cm thin-layered quartz glass cell using platinum wire as counter electrode and SCE as reference electrode using BMIM TFSI as supporting liquid electrolyte. A PC-controlled VSP-Potentiostat synchronized with a monolithic miniature spectrometer (MMS) UV–vis high speed diode array spectrometer with a bandwidth of 300–1100 nm and a deuterium/ tungsten light source coupled to an optical fiber was employed to register the spectra. BioKine32 software was used for data acquisition and treatment. Indium tin oxide (ITO) electrodes



SCHEME 1 | Synthetic routes to *N*-phenylcarbazoles **1** and **4**.

on flexible PET substrate (ref. DRP-ITO10) were acquired from Metrohm DropSens and used to study electrochemical and spectroelectrochemical behaviour respectively of electrodeposited NPC polymer using solid gel BMIM-TFSI as proof of concept to demonstrate the feasibility of the system to be implemented in real flexible electrochromic devices. Nuclear magnetic resonance (NMR) spectra were obtained employing Bruker spectrometers DPX-250, DXP-360 and AVANCE-III 400 (Servei de Resonància Magnètica Nuclear; Universitat Autònoma de Barcelona) (250 MHz (^1H); 62.5 MHz (^{13}C), 360 MHz (^1H); 90 MHz (^{13}C) and 400 MHz (^1H); 100 MHz (^{13}C)). ^1H and ^{13}C chemical shifts are reported in ppm relative to tetramethylsilane, using residual proton and ^{13}C resonances from solvent as internal standards.

2.2 | Monomer Synthesis

4-(9*H*-carbazol-9-yl)phenol (**1**) and 4-(3-methoxy-9*H*-carbazol-9-yl)phenol (**4**) were synthesized following the procedures previously described in the literature for similar compounds using a Schlenk set-up when required (Scheme 1):

4-(9*H*-carbazol-9-yl)phenol (1): In 20 mL of a 95% ethanol solution under continuous stirring were suspended commercial 4-(diphenylamino)phenylboronic acid (0.50 g, 1.26 mmol), 3 equivalents of $\text{NH}_2\text{OH}\cdot\text{HCl}$ (0.26 g, 3.80 mmol) and 4 equivalents of NaOH (0.20 g, 5.00 mmol) at room temperature. After 24 h, 20 mL of CH_2Cl_2 were added and the solvents were eliminated under reduced pressure. The solid obtained was solved in 30 mL of CH_2Cl_2 and washed with water (3×30 mL). When the aqueous phase reached a pH of 4 by adding HCl 2 M, the organic part was extracted with 30 mL (x 2) de CH_2Cl_2 . Finally, the organic phases were collected, and the solvent was dried with anhydrous Na_2SO_4 , filtered and the solvent evaporated under

reduced pressure. The solid **1** (0.31 g, 96%) was obtained by silica column chromatography 8:2 v/v hexane: ethyl acetate [32]. $^1\text{H-NMR}$ (acetone- d_6 , 400 MHz) δ (ppm): 8.91 (s, 1H), 8.18 (d, $J = 7.8$ Hz, 2H), 7.41-7.37 (m_{ap}, 4H), 7.31 (d, $J = 8.2$ Hz, 2H), 7.24 (t, $J = 7.4$ Hz, 2H), 7.14 (d, $J = 8.7$ Hz, 2H).

3-methoxy-9*H*-carbazol (2): Pivalic acid (4.5 g, 44.06 mmol), 4-methoxy-*N*-phenylamine (1.0 g, 5 mmol), palladium acetate (0.056 g, 0.25 mmol) and potassium carbonate (0.069 g, 0.5 mmol) were mixed and heated at 110°C under continuous stirring during 14 h. After this time, 50 mL of CH_2Cl_2 were added and the crude was washed with a saturated solution of Na_2CO_3 (125 mL). The resulting organic phase was dried with anhydrous Na_2SO_4 , filtered and the solvent evaporated under reduced pressure. The product **2** (0.43 g, 43%) was purified by silica column chromatography 8:2 v/v hexane: ethyl acetate [33]. $^1\text{H-NMR}$ (DMSO- d_6 , 360 MHz) δ (ppm): 11.03 (s, NH), 8.09 (d, $J = 7.8$ Hz, 1H), 7.67 (d, $J = 2.5$ Hz, 1H), 7.44 (d, $J = 8.1$ Hz, 1H), 7.39 (d, $J = 8.7$ Hz, 1H), 7.34 (d, $J = 7.6$ Hz, 1H), 7.10 (t_{ap}, $J = 7.6$ Hz, 1H), 7.02 (dd, $J_1 = 8.7$ Hz, $J_2 = 2.5$ Hz, 1H), 3.84 (s, 3H).

(4-bromophenoxy)(*tert*-butyl)dimethylsilane (3): In a Schlenk type flask were dried 4-bromophenol (0.60 g, 3.47 mmol), *tert*-butyldimethylsilyl chloride (0.92 g, 6.10 mmol) and imidazole (0.59 g, 8.75 mmol) under reduced pressure for 15 min. Over this mixture dichloromethane was added and stirred under nitrogen atmosphere one hour. After this time, 20 mL of CH_2Cl_2 was added to the reaction and the crude was washed three times with 30 mL of water. The organic phase was dried with anhydrous Na_2SO_4 , filtered and the solvent evaporated under reduced pressure to give compound **3** as a pure transparent liquid (0.83 g, 83%) [18, 34]. $^1\text{H-NMR}$ (CDCl_3 , 360 MHz) δ (ppm): 7.32 (d, $J = 8.7$ Hz, 2H), 6.72 (d, $J = 8.7$ Hz, 2H), 0.97 (s, 9H), 0.18 (s, 6H).

4-(3-methoxy-9H-carbazol-9-yl)phenol (4): In a Schlenk type flask were dried 3-methoxy-9H-carbazole (0.57 g, 2.90 mmol), (4-bromophenoxy)(*tert*-butyl)dimethylsilane (0.83 g, 2.90 mmol), palladium acetate (3.00 mg, 0.013 mmol) and sodium *tert*-butoxide (0.74 g, 7.70 mmol) at 2 mbar during 20 min. Then 10 mL of anhydrous toluene were introduced to the mixture. Over this solution, under argon atmosphere, tri-*tert*-butylphosphine (0.04 g, 0.20 mmol) were added and the reaction crude was refluxed 5 h. After this time, the crude was cooled down and the solvent evaporated under reduced pressure. The resulting solid was solved in 50 mL of ethyl acetate and washed three times with brine (40 mL) and twice with pure water (30 mL). The organic phase was dried with anhydrous Na₂SO₄ and filtered. Then, the solvent was evaporated under reduced pressure. The solid obtained (0.40 g, 0.99 mmol) was directly treated with tetra-*n*-butylammonium fluoride (0.94 g, 2.97 mmol) in 5 mL of THF. After 40 min, 30 mL of ethyl acetate were added to the solution and the resulting mixture was washed with 40 mL of brine/water 50/50 v/v (x3). After dried with anhydrous Na₂SO₄ and filtered, the solvent was removed and the solid was purified by silica column chromatography 9:1 v/v hexane: ethyl acetate giving the compound **4** (0.093 g, 11%) [35, 36]. ¹H-NMR (CDCl₃, 360 MHz) δ (ppm): 8.10 (d, $J = 7.8$ Hz, 1H), 7.63 (d_{asim}, $J = 2.5$ Hz, 1H), 7.40-7.38 (m_{ap}, 3H), 7.32 (d_{asim}, $J = 8.0$ Hz, 1H), 7.26-7.23 (m_{ap}, 2H), 7.07-7.02 (m_{ap}, 3H), 3.96 (s, 3H).

2.3 | Electropolymerization and Spectroelectrochemical Characterization Procedure of NPC-based Polymers P1 and P4

Electrochemical polymerization and spectroelectrochemical characterization of **P1** and **P4** were performed in thermostated cell at 22 °C, with no requirement for inert atmosphere.

Electrodeposition of poly[4-(9H-carbazol-9-yl)phenol] (**P1**) and poly[4-(3-methoxy-9H-carbazol-9-yl)phenol] (**P4**) were performed using a 5 mL solutions containing 18.2 mM of monomer **1** and 10 mM of monomer **4**, respectively in BMIM TFSI. ITO-PET was used as the WE previously masked with parafilm to expose 2x1 cm² effective area. The WE, CE (Pt wire) and reference (SCE) electrodes were then placed in a conical electrochemical cell and immersed in the corresponding monomer solution. A constant potential of 1.60 V versus SCE was applied until the initial current decreased by 80% and 50% for **P1** and **P4** respectively (Scheme 2).

To electrochemically characterize the polymer films formed three replicates of **P1** and **P4** were prepared ($n = 3$) and negligible deviation were observed for both cases. CV were performed using fresh BMIM TFSI and the ITO-PET WE with previously electrodeposited **P1** and **P4** over a potential scan sweep from 0.0 to 3.0 V at 0.1 V s⁻¹ scan rate. The electrochemical cycling resistance of the polymers was evaluated by CA, applying 50 consecutive oxidation-reduction potential steps of 0 and 2.5 V versus SCE, for 30 s each.

P1 and **P4** were also electrodeposited, following the same procedure onto a screen-printed and flexible ITO-PET acquired from Metrohm Dropsens and using an ionogel based on BMIM TFSI as solid-gel electrolyte in order to demonstrate the feasibility of

a fully flexible integrated ECD. The ionogel was easily prepared in-house following a previously reported procedure [37].

Finally, spectroelectrochemical measurements of **P1** and **P4** films ($n = 3$) were performed by recording the UV-Vis spectra in the 300–1000 nm range using a quartz cell with a 0.1 cm optical path length. A constant oxidation potential of 2.50 V for P1 and 1.80 V for P4 versus SCE was applied and 0 V versus SCE was applied to convert the polymer back to the neutral form for both cases. The spectroelectrochemical cycling stability study of **P1** and **P4** was also evaluated by recording the time-dependent absorbance spectra while applying alternating oxidation and reduction potentials for 120 s each. Depending on the configuration used, either liquid BMIM TFSI IL or a BMIM TFSI-based ionogel electrolyte was employed.

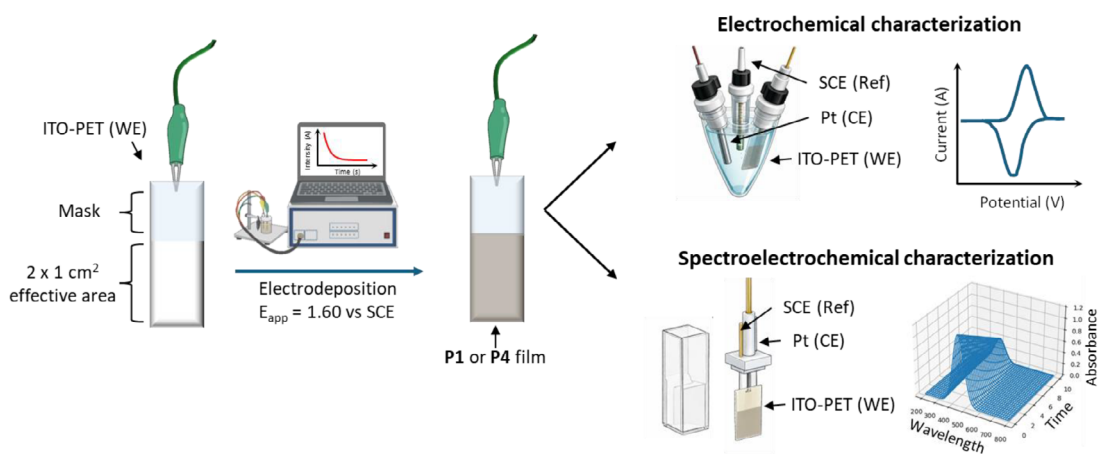
3 | Results and Discussion

3.1 | Electropolymerization of NPCs

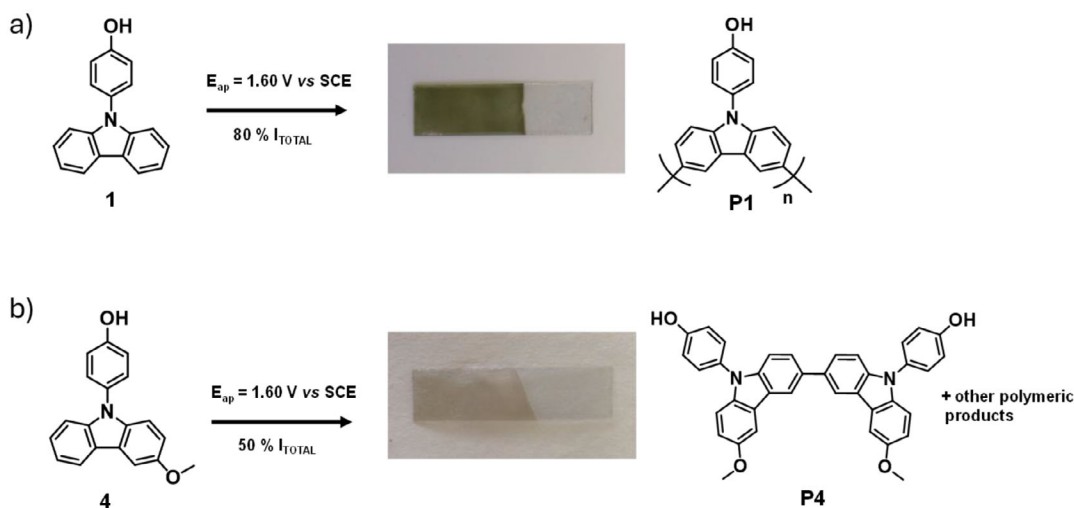
Electrochemical polymerization of both compounds (**1**, **4**) (Scheme 3) were carried out using a reaction medium containing 18.2 mM of **1** or 10 mM of **4** in BMIM TFSI. The polymeric film was deposited by amperometry onto the ITO-PET electrode immersed in the corresponding monomeric solution.

For monomer **1** a constant potential of 1.60 V versus SCE was applied until the current decreased to 80% of its initial value, ensuring predominantly faradaic current and avoiding undesired side reactions. This potential value, slightly above the anodic peak potential (E_{pa}), was chosen considering that the E_{pa} of the phenylcarbazole structure in solution was 1.18 V versus SCE. At this point, a green film was uniformly formed on ITO-PET electrode surface immersed in the monomer solution (Scheme 3a) with no apparent defects in the films. Upon oxidation, monomer **1** is converted to its dication, which subsequently undergoes a coupling reaction at the two unsubstituted para positions of the carbazole unit, leading to the formation of carbon-carbon bonds between adjacent monomers. As the polymer chains grow, the resulting electroactive N-phenylcarbazole-based polymer (**P1**) is electrodeposited onto the ITO-PET electrode surface.

Electropolymerization of compound **4** was carried out under the same conditions. However, the chronoamperometric oxidation at 1.60 versus SCE was halted when the intensity current decreased to 50% of its initial value (Scheme 3b) in order to have a control of film thickness and avoid film detachment resulting from uncontrolled film growth. In this case, the presence of the substituent -methoxy group- on the aromatic ring blocks one of the two *para* positions of the carbazole unit. As a result, only a single position remains available for oxidative coupling reaction which restricts the reaction pathway to the formation of dimers through the coupling of two oxidized monomer units. Consequently, the electrochemical process is expected to proceed predominantly through the formation of dimers, as further chain propagation is sterically and electronically hindered. However, after the oxidation process at constant potential, a film **P4** was also formed on the surface of the electrode similarly to what was observed for compound **1**. This result suggests that in this electrochemical condition the monomer **4** is capable of under-



SCHEME 2 | On the left, schematic representation of an ITO–PET electrode are masked to limit the effective electrode area on which **P1** and **P4** films are electrodeposited at constant potential. On the right: electrochemical and spectroelectrochemical characterization, showing the experimental setups used for the characterization of the formed **P1** and **P4** films.



SCHEME 3 | Electropolymerization of (a) **1** and (b) **4** from a solution of monomers to obtain polymeric films **P1** and **P4** respectively onto ITO–PET flexible electrode. Note than only exposed.

going coupling reactions at positions other than the preferred para positions. Additionally, the aromatic and planar nature of the carbazole framework may promote π – π stacking interactions, which can stabilize radical cation intermediates and facilitate the proximity required for these alternative coupling pathways.

The results demonstrate that electropolymerization enables the efficient formation of thin polymer films based on polycarbazole derivatives directly on flexible, optically transparent ITO–PET electrodes. The films obtained exhibit good adhesion and electroactivity, confirming the suitability of this IL-based approach for fabricating polymer layers on flexible substrates.

3.2 | Electrochemical Characterization of Electro-generated Polymers **P1** and **P4**

Electrochemical behavior of both polymer films (**P1** and **P4**) was characterized by CV, at 22 °C using fresh BMIM TFSI as an

ecofriendly supporting electrolyte in a conical electrochemical cell, a platinum bar CE and SCE reference electrode. **P1** showed an E_{pa} at 1.77 V (Figure 1a) and **P4** at 2.18 V versus SCE (Figure 1b). The observed electrochemical behaviour upon oxidation can be attributed, in both cases, to the formation of radical cations of the *N*-phenylcarbazole units that constitutes the polymer backbone. In the reverse cathodic scan, a reduction peak appears at 0.5 V and 0.0 V versus SCE for **P1** and **P4**, respectively, corresponding to the reversible reduction of the oxidized species to the neutral form of the polymer film.

The electrochemical cycling resistance of **P1** and **P4** was also studied by applying 50 oxidation–reduction cycles (0–2.5 V versus SCE) of 30 s each using BMIM TFSI as electrolyte solution as before (Figure 1c,d). **P1** retained 100% of its electrochemical response after 50 cycles, while **P4** maintained 97% of its initial current intensity with an error range of $\approx 3\%$, with no delamination or defects observed, indicating excellent electrochemical robustness and redox stability.

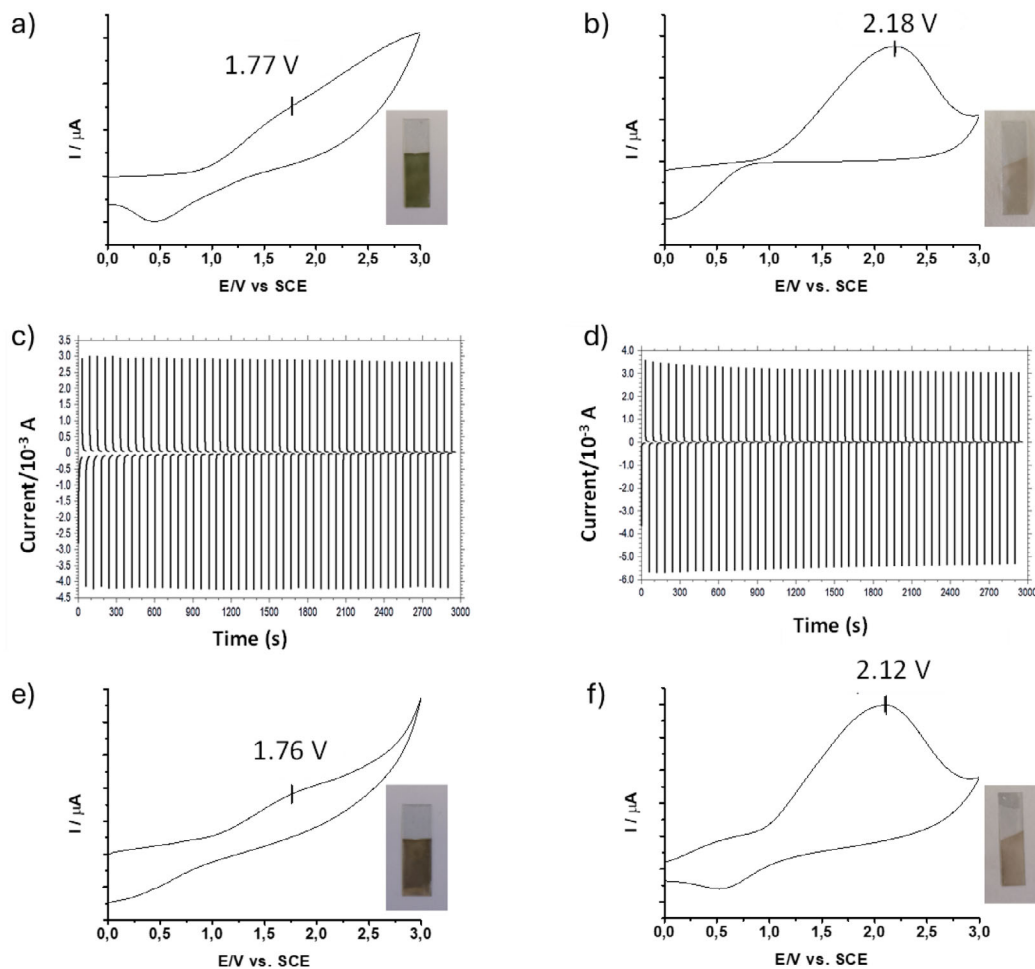


FIGURE 1 | CV of the initial (a) **P1** and (b) **P4** and the visual aspect of the electrodeposited ITO-PET electrodes. CA of 50 consecutive oxidation-reduction cycles of (c) **P1** and (d) **P4** when applying 0–2.5 V versus SCE for 30 s. CV of (e) **P1** and (f) **P4** after the redox cycles and their visual appearance.

After the electrochemical resistance test, a CV was recorded in fresh BMIM TFSI to confirm that no chemical changes occurred, and thus a change that the electrochemical response remained unchanged. The results (Figure 1e,f) revealed no significant differences between the response of the initial voltammograms and those recorded after the redox cycles with comparable anodic peaks potentials. Additionally, the visual appearance of the films deposited on the ITO-PET remained unchanged, indicating that no delamination, discoloration, or surface degradation occurred during the electrochemical treatment.

These results confirm the high reversibility and robustness of both polymeric systems, **P1** and **P4**, under repeated cycling, which is particularly relevant for their potential application in electroactive devices, where long-term operational stability is crucial. The minimal loss in performance suggests that the redox processes involved are highly reversible and do not lead to significant structural or chemical degradation of the polymer films.

3.3 | Electrochromic Properties of Polymers **P1** and **P4**

After the successful formation of **P1** and **P4** onto flexible ITO-PET electrodes, their electrochromic behaviour was thoroughly

investigated. Spectroelectrochemical measurements were performed to monitor the potential-induced optical changes in the materials. This approach enabled real-time tracking of their spectral evolution across the UV-Vis to near-NIR regions, providing valuable insights into the electronic transitions and charge carrier dynamics associated with their redox states.

As mentioned in the previous section, the electropolymerization conditions of **P1** and **P4** were accurately adjusted, particularly in view of the critical role of transparency in the NIR region. For this reason, electropolymerization of **P1** and **P4** was carried out until 80% and 50% of the initial current, respectively, had passed to obtain controlled polymer thickness. On the one hand, thick layers are prone to poor adhesion and become opaque, hindering complete color switching, whereas thin films fail to provide sufficient optical contrast.

Based on these considerations, ITO-PET electrodes modified with **P1** and **P4** presented different electro-optical behaviors, each exhibiting a broad absorbance band observed in the NIR region during the oxidation process in BMIM TFSI electrolyte. **P1** showed a spectroscopic response at 1000 nm only at high applied potential (2.50 V versus SCE). In contrast, **P4** required a lower anodic applied potential (1.80 versus SCE), which is attributed to its *N*-phenylcarbazole-enriched structure bearing

TABLE 1 | Electrochromic parameters of **P1** and **P4** on ITO-PET in BMIM TFSI.

Polymer	λ_{\max} (nm)	$\Delta T\%$ ^a	t_c (s)	t_d (s)	ΔOD	Q (mC)	A (cm ²)	Π (cm ² /C) ^b	Γ (mol/cm ²)
P1	1000	3	75	82	0.007	0.32	1.48	31	$2.4 \cdot 10^{-9}$
P4 ^c	782	9	57	46	0.042	3.35	1.36	17	$2.5 \cdot 10^{-8}$

^aSimilar polymers present values of 17–43% at close maximum wavelength [43, 44];

^bsimilar polymer present values of 48 cm²/C at close maximum wavelength [44];

^cdata obtained from redox cycle n°5.

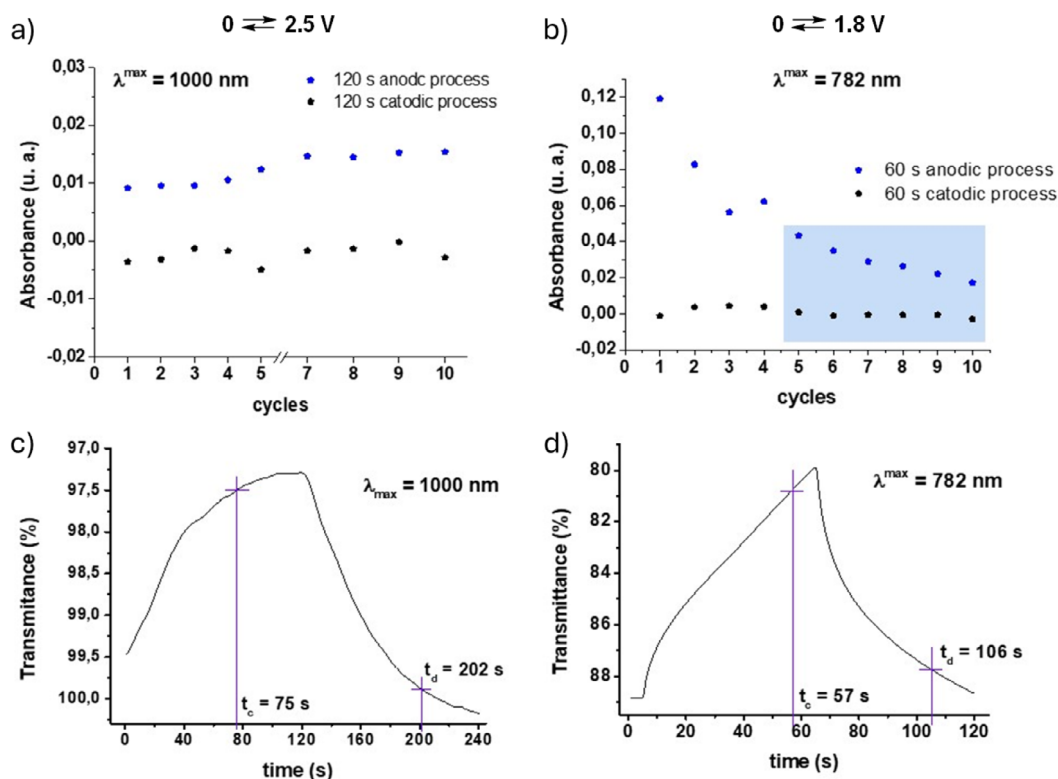


FIGURE 2 | Absorbance versus number of cycles (oxidation-reduction) realized at (a) 1000 nm for **P1** and (b) 782 nm for **P4**. Transmittance (%) versus time representation of the oxidation process at a maximum wavelength of (c) 1000 nm for **P1** and (d) 782 nm for **P4**.

two electron-donating substituents [38, 39]. Applying this potential to the **P4**-modified ITO-PET electrode resulted in a maximum absorbance band at 782 nm.

Besides, the theoretical surface coverage of **P1** and **P4** was calculated from the charge (Q) consumed during electropolymerization and the area (A) of the deposited film on the ITO-PET, the number of electrons involved in the electron transfer (n) and the Faradaic constant (F). The covering (Γ) in mol cm⁻² was calculated for each material ($\Gamma = (Q/nFA)$) (Table 1), which was $2.24 \cdot 10^{-9}$ mol cm⁻² for **P1** and $2.5 \cdot 10^{-8}$ mol cm⁻² for **P4**. This parameter allows not only control over film thickness growth but fine-tuning the electrochromic performance. In particular, controlling the coverage of **P1** and **P4** is crucial, as the electrochromic properties are highly dependent on the thickness and uniformity of the films.

In addition, the electro-optic fatigue resistance of the films was investigated. As depicted in Figure 2a, the absorbance of **P1** along each oxidation-reduction cycle remains nearly constant for at

least 10 cycles at a wavelength of 1000 nm. This indicates the electrochromic stability and reversibility of **P1** on the ITO-PET electrode in BMIM TFSI over 10 cycles.

On the other hand, the absorbance-cycles representation for **P4** showed a continuous decrease in the absorbance upon the oxidation potential up to 5 cycles. (Figure 2b). Thus, **P1** and **P4** cycling measurements demonstrated stability within $\pm 3 - 5\%$ variation range. Although the **P4** system is advantageous compared to **P1** due to the lower potential required to induce a change in the IR absorbance, it seems that some low-molecular-weight **P4** chains were not well anchored to the electrode and detached during the redox cycles until reaching a stable layer (Figure 2b, blue zone).

The spectroelectrochemical analysis also allowed us to determine the electrochromic parameters for each *N*-phenylcarbazole polymer, considering that the covering is an order of magnitude higher for **P4**, which in principle leads to greater electrochromic performance values [40].

3.4 | Optical Contrast (ΔT %)

The optical contrast, defined as the difference in transmittance (ΔT %) between the bleached and colored states at a specific wavelength, was obtained from the electrochromic switching studies for the electroactive polymers. This value was 3% for **P1** at 1000 nm and 9% for **P4** at 782 nm. It is well known the relationship between the thickness of the electrochromic polymer layer and the optical contrast achieving greater values with higher covering of the electrode.

3.5 | Response Time (t)

The response time is defined as the time required for an electrochromic material to achieve 90% of the total change in transmittance at a specific wavelength [16, 41]. Figure 2 shows the oxidation-reduction profile for 120 s each, represented as transmittance (%) versus time (s) with the 90% transmittance threshold for each process is highlighted in purple. Conversely, the time needed for the reduction process was 82 s for **P1** and 46 s for **P4** (Table 1). Although these values may initially seem elevated for a colour-switching process, they are significantly shorter than those typically reported for smart window applications, where commercial systems often require response times on the order of several minutes. This demonstrates the strong potential of our approach for enhancing electrochromic device efficiency following a green process and suitability for real-world integration [42].

3.6 | Coloration Efficiency (η)

The coloration efficiency (η) is defined as the change in the optical density ($\Delta OD = \log(T_d/T_c)$), and was calculated from the ratio of the transmittance at decolorized (T_d) or reduced state to that in the colored (T_c) or oxidated state, normalized by the electric charge applied (Q_d) which is the charge consumed during the process divided by the area covered by the electrochromic material ($\eta = \Delta OD/Q_d$). For this parameter, the less charge required for the coloration change, the better the electrochromic performance. The coloration efficiency was determined to be 31 $\text{cm}^2 \text{C}^{-1}$ for **P1** at 1000 nm and 17 $\text{cm}^2 \text{C}^{-1}$ for **P4** at 782 nm.

These coloration efficiency values compare favourably with typical values reported for organic electrochromic polymers in the visible and near-infrared regions, which generally range from 10 to 50 $\text{cm}^2 \text{C}^{-1}$ [6, 7]. These results highlight the potential of NPC-based electrochromic films for practical applications such as smart windows and IR modulators. Moreover, our approach offers the advantage of a greener and simpler material preparation process, making these films attractive candidates for sustainable device applications.

3.7 | Construction of NPC-based Display for Greener Electrochromic and Flexible Applications

The electropolymerization behavior of the NPC **P1** was studied using a simple device based on a flexible screen-printed electrode with BMIM TFSI based ionogel (Figure 3). This electrode consists

of a polyethylene terephthalate (PET) substrate on which a three-electrode system is printed: the working electrode based on ITO, the Ag/AgCl reference electrode and the counter electrode printed as graphite. To monitor the electropolymerization process, 50 μL drop of a 18.2 mM solution of monomer **1** in BMIM-TFSI was placed on the electrode surface and a constant potential of 1.60 V versus Ag/AgCl was applied during 180 s while the optical response was recorded by spectroelectrochemistry. In Figure 3a, the color change produced by the electropolymerization process, from colorless to pale green, is clearly observed. This phenomenon is supported by the spectrum presented in Figure 3b which a progressive increase in the absorption bands located at 420 and 1000 nm concurrent with the growth of the polymer layer. These spectral changes are indicative of enhanced charge delocalization and mobility along the oxidized polymer chains. This experiment thereby validates the feasibility of fabricating straightforward electrochromic devices through the in-situ generation of electro-optically active polymer films. Additionally, qualitative flexibility tests were carried out by manually bending the electrode, and no noticeable changes in the electrochromic response were observed, suggesting good mechanical robustness and structural uniformity of the polymer film on the flexible substrate.

4 | Conclusion

In this work, two monomeric derivatives of NPC, **1** and **4**, were successfully synthesized, providing a promising platform for low-potential electropolymerization of electroactive polymers directly onto transparent and flexible ITO-PET substrates. Notably, the electropolymerization process was carried out in BMIM TFSI, an IL electrolyte, completely avoiding the use of traditional hazardous organic solvents and salts. This greener and more sustainable approach enhances the environmental compatibility and reusability of the system, aligning with the growing trend towards eco-friendly fabrication methods in advanced device manufacturing.

The resulting electroactive films exhibited promising surface coverages of $2.24 \cdot 10^{-9}$ and $2.5 \cdot 10^{-8}$ mol cm^{-2} , respectively, demonstrating efficient material deposition on flexible electrodes. Electrochromic characterization revealed competitive performance, with coloration efficiencies of 31 and 17 $\text{cm}^2 \text{C}^{-1}$, highlighting the strong electro-optical response of the polymers. Notably, polymer **P1** showed superior coloration efficiency despite lower surface coverage, indicating enhanced electrochromic activity per charge injected and potential for optimization through thickness and morphology control. On the other hand, **P4** demonstrated the capability of NPC to shift to lower potentials by tuning pendant groups in the polymer chain, opening the door to a more varied family of NPC that would enable the fabrication of low-powered ECDs.

Both systems maintained electrochemical stability over multiple redox cycles, confirming their suitability for flexible device applications. These results advance sustainable fabrication strategies for electrochromic materials and demonstrate the viability of ionic-liquid-assisted electropolymerization as a scalable route toward high-performance, environmentally compatible electrochromic devices.

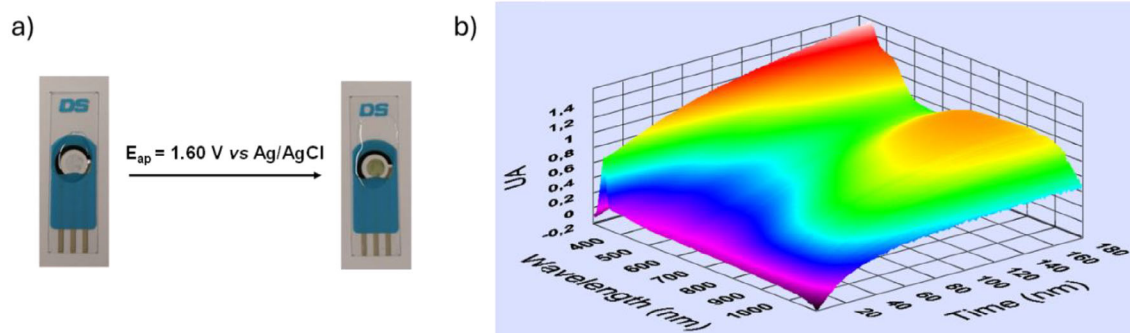


FIGURE 3 | (a) Color evolution of the electropolymerization of monomer **1** in BMIM TFSI ionogel-based at an oxidation potential of 1.60 V versus Ag/AgCl; (b) 3D spectroelectrochemical absorbance spectrum over time recorded when applying 1.60 V versus Ag/AgCl at the BMIM-TFSI- monomer **1** solution during 180 s.

Acknowledgments

We gratefully acknowledge the financial support from the Spanish Ministry of Innovation, Science and Universities (MICIU/AEI/10.13039/501100011033 and ERDF—“A way of making Europe”) through grants PID2019-106171RB-I00 and PID2022-141293OB-I00. In addition, the authors thanks AGAUR (Generalitat de Catalunya (2021 SGR 00064 and 2021 SGR 00052)). C.G. and also to the Spanish Ministry of Science, Innovation and Universities for the award of a research studentship via the FPI program (BES-2016-078179). S.S. acknowledges support from the Horizon Europe Marie Skłodowska-Curie Postdoctoral Fellowship HORIZON-MSCA-2023-PF-01 (Grant Agreement No. 101152453 — PON-SXT).

Conflicts of Interest

The authors declare no conflicts of interest.

Data Availability Statement

The data analyzed during the current study are available from the corresponding authors.

References

1. T. M. Benedetti, T. Carvalho, D. C. Iwakura, et al., “All Solid-state Electrochromic Device Consisting of a Water Soluble Viologen Dissolved in Gelatin-based Ionogel,” *Solar Energy Materials and Solar Cells* 132 (2015): 101.
2. V. K. Thakur, G. Ding, J. Ma, P. S. Lee, and X. Lu, “Hybrid Materials and Polymer Electrolytes for Electrochromic Device Applications,” *Advanced Materials* 24 (2012): 4071.
3. A. Kavanagh, K. J. Fraser, R. Byrne, and D. Diamond, “An Electrochromic Ionic Liquid: Design, Characterization, and Performance in a Solid-state Platform,” *ACS Applied Materials & Interfaces Journal* 5 (2013): 55.
4. P. M. S. Monk, R. J. Mortimer, and D. R. Rosseinsky, *Electrochromism and Electrochromic Devices* (Wiley VCH Verlag GmbH, 2007).
5. D. R. Rosseinsky and R. J. Mortimer, “Electrochromic Systems and the Prospects for Devices,” *Advanced Materials* 13 (2001): 783.
6. R. J. Mortimer, “Electrochromic Materials,” *Annual Review of Materials Research* 41 (2011): 241.
7. P. M. Beaujuge and J. R. Reynolds, “Color Control in π -Conjugated Organic Polymers for Use in Electrochromic Devices,” *Chemical Reviews* 110 (2010): 268–320.

8. B. B. Carbas, “Fluorene-Based Electrochromic Conjugated Polymers: A Review,” *Polymer* 254 (2022): 125040.
9. B. B. Carbas, E. G. C. Ergun, and S. O. Hacioglu, “Electrochromic Properties of Carbazole-based Electrodeposited Copolymers: A Review,” *Chemical Engineering Journal* 526 (2025): 169629.
10. F. Bekkar, F. Bettahar, I. Moreno, et al., “Polycarbazole and Its Derivatives: Synthesis and Applications A Review of the Last 10 Years,” *Polymers* 12 (2020): 2227.
11. D. Witker and J. R. Reynolds, “Soluble Variable Color Carbazole-Containing Electrochromic Polymers,” *Macromolecules* 38 (2005): 7636–7644.
12. P. M. Beaujuge and J. R. Reynolds, “Color Control in π -conjugated Organic Polymers for Use in Electrochromic Devices,” *Chemical Reviews* 110 (2010): 268.
13. G. Gunbas and L. Toppare, “Electrochromic Conjugated Polymers,” *Chemical Communications* 48 (2012): 1083.
14. S.-H. Hsiao and J.-C. Hsueh, “Electrochemical Synthesis and Electrochromic Properties of New Conjugated Polycarbazoles From Di(carbazol-9-yl)-substituted Triphenylamine and *N*-phenylcarbazole Derivatives,” *Journal of Electroanalytical Chemistry* 758 (2015): 100.
15. B. B. Carbas and H. B. Yildiz, “A Review of dithieno[3,2-b:2',3'-d]Pyrrole-based Electrochromic Conjugated Polymers,” *European Polymer Journal* 204 (2024): 112700.
16. S. Zhang, G. Sun, Y. He, R. Fu, Y. Gu, and S. Chen, “Preparation, Characterization, and Electrochromic Properties of Nanocellulose-based Polyaniline Nanocomposite Films,” *ACS Applied Materials and Interfaces* 9 (2017): 16426.
17. B. B. Carbas, “Disruptive Electrochromic Materials: Carbazole-Based Conjugated Polymers,” *ACS Applied Polymer Materials* 7 (2025): 4051–4076.
18. F. Liang, T. Kurata, H. Nishide, and J. Kido, “Synthesis and Electrochemical and Electroluminescent Properties of *N*-phenylcarbazole-substituted Poly(*p*-phenylenevinylene),” *Journal of Polymer Science* 43 (2005): 5765.
19. J. Qu, D. Li, Y. Chen, and X. Shen, “Synthesis and Properties of Polyacetylenes Carrying *N*-phenylcarbazole and Triphenylamine Moieties,” *Polymer* 47 (2006): 8940.
20. A. Brazier, G. B. Appetecchi, S. Passerini, et al., “Ionic Liquids in Electrochromic Devices,” *Electrochimica Acta* 52 (2007): 4792–4797.
21. S. Zanarini, N. Garino, J. R. Nair, et al., “Contrast Enhancement in Polymeric Electrochromic Devices Encompassing Room Temperature Ionic Liquids,” *International Journal of Electrochemical Science* 9 (2014): 1650–1662.

22. B. Bezgin Carbas and B. Tekin, "Poly(3,4-ethylenedioxythiophene) Electrode Grown in the Presence of Ionic Liquid and Its Symmetrical Electrochemical Supercapacitor Application," *Polymer Bulletin* 75 (2018): 1547–1562.
23. M. Ak and R. Ayranci, "Unique and Efficient Modulation of Polycarbazole Thin Film Surface Morphology by Electrochemical, Photochemical and Self-assembly Techniques," *Materials Today* 42 (2024): 102379.
24. R. Kirankumar, W. Huang, H. Chen, and P. Chen, "Electropolymerization and Characterization of Carbazole Substituted Viologen Conducting Polymers: The Effects of Electrolytes and Potential Applications of the Polymers," *Journal of Electroanalytical Chemistry* 826 (2018): 198.
25. T. Abidin, Q. Zhang, K.-L. Wang, and D.-J. Liaw, "Recent Advances in Electrochromic Polymers," *Polymer* 55 (2014): 5293–5304.
26. B. B. Carbas, S. Özbakır, and Y. Kaya, "A Comprehensive Overview of Carbazole-EDOT Based Electrochromic Copolymers: A New Candidate for Carbazole-EDOT Based Electrochromic Copolymer," *Synthetic Metals* 293 (2023): 117298.
27. E. G. C. Ergun and B. B. Carbas, "Electrochromic Copolymers of 2,5-dithienyl-N-substituted-pyrrole (SNS) Derivatives With EDOT: Properties and Electrochromic Device Applications," *Materials Today Communications* 32 (2022): 103888.
28. D. Nunes, T. Freire, A. Barranger, et al., "TiO₂ Nanostructured Films for Electrochromic Paper-Based Devices," *Applied Sciences* 10 (2020): 1200.
29. P. Duarte, S. Pereira, I. Cunha, et al., "Cellulose-Based Solid Electrolyte Membranes through Microwave Assisted Regeneration and Application in Electrochromic Displays," *Frontiers in Materials* 7 (2020): 269.
30. B. B. Carbas and E. G. C. Ergun, "A Classified and Comparative Review of Poly(2,5-dithienyl-N-substituted-pyrrole) Derivatives for Electrochromic Applications," *European Polymer Journal* 175 (2022): 111363.
31. D. Bradley, G. Williams, and M. Lawton, "Drying of Organic Solvents: Quantitative Evaluation of the Efficiency of Several Desiccants," *Journal of Organic Chemistry* 75 (2010): 8351.
32. E. Kianmehr, M. Yahyae, and K. Tabatabai, "A Mild Conversion of Arylboronic Acids and Their Pinacolyl Boronate Esters Into Phenols Using Hydroxylamine," *Tetrahedron Letters* 48 (2007): 2713.
33. B. Liégault, D. Lee, M. P. Huestis, D. R. Stuart, and K. Fagnou, "Intramolecular Pd(II)-catalyzed Oxidative Biaryl Synthesis Under Air: Reaction Development and Scope," *Journal of Organic Chemistry* 73 (2008): 5022.
34. A. Bartoszewicz, M. Kalek, J. Nilsson, R. Hiresova, and J. Stawinski, "A New Reagent System for Efficient Silylation of Alcohols: Silyl Chloride-N-methylimidazole-iodine," *Synlett* 1 (2008): 37.
35. Y. Sun, N. Zhou, W. Zhang, et al., "Synthesis of Novel Side-chain Triphenylamine Polymers With Azobenzene Moieties via RAFT Polymerization and Investigation on Their Photoelectric Properties," *Journal of Polymer Science Part A: Polymer Chemistry* 50 (2012): 3788.
36. E. J. Corey and A. Venkateswarlu, "Protection of Hydroxyl Groups as *Tert*-butyldimethylsilyl Derivatives," *Journal of American Chemistry Society* 94 (1972): 6190.
37. S. Santiago, X. Muñoz-Berbel, and G. Guirado, "Study of P(VDF-co-HFP)-ionic Liquid Based Ionogels for Designing Flexible Displays," *Journal of Molecular Liquids* 318 (2020): 114033.
38. P. Cias, C. Slugovc, and G. Gescheidt, "Hole Transport in Triphenylamine-based OLED Devices: From Theoretical Modeling to Properties Prediction," *Journal of Physical Chemistry A* 115 (2011): 14519.
39. P. Winget and J.-L. Brédas, "Ground-state Electronic Structure in Charge-transfer Complexes Based on Carbazole and Diarylamine Donors," *Journal of Physical Chemistry C* 115 (2011): 10823.
40. J. Niu, Y. Wang, X. Zou, et al., "Infrared Electrochromic Materials, Devices and Applications," *Applied Materials Today* 24 (2021): 101073.
41. R. Lakshmanan, P. Raja, N. Shivaprakash, and S. Sindhu, "Fabrication of Fast Switching Electrochromic Window Based on Poly(3,4-(2,2-dimethylpropylenedioxy)Thiophene) Thin Film," *Journal of Materials Science: Materials in Electronics* 27 (2016): 6035.
42. A. Cannavale, U. Ayr, F. Fiorito, and F. Martellotta, "Smart electrochromic windows to enhance building energy efficiency and visual comfort," *Energies* 13 (2020): 1449.
43. S. Koyuncu, B. Gultekin, C. Zafer, et al., "Electrochemical and Optical Properties of Biphenyl Bridged-dicarbazole Oligomer Films: Electropolymerization and Electrochromism," *Electrochimica Acta* 54 (2009): 5694.
44. S. H. Hsiao and S. W. Lin, "Electrochemical Synthesis of Electrochromic Polycarbazole Films From N-phenyl-3,6-bis(N-carbazolyl)Carbazoles," *Polymer Chemistry* 7 (2016): 198.